General aspects of hydrodynamic interactions between three-sphere low-Reynolds-number swimmers

Majid Farzin,* Kiyandokht Ronasi, and Ali Najafi
Department of Physics, Zanjan University, Zanjan 313, Iran
(Received 25 February 2012; revised manuscript received 21 May 2012; published 19 June 2012)

We investigate hydrodynamic interactions between two three-sphere swimmers analytically and numerically. Hydrodynamic forces exerted on the swimmers as well as the translational and angular velocities of them are obtained in the far field regime. We demonstrate that the active term of the translational velocity is along the intrinsic direction of swimming ($\mathbf{n}$) and has no component along the direction of relative positions of swimmers ($\hat{\mathbf{r}}$) as reported in previous papers. Using numerical simulations we investigate the long-time swimming paths of swimmers in two general situations of swimming in the same and opposite directions. The former reveals four swimming states for symmetric swimmers—attractive, repulsive, parallel, and oscillatory—and only three swimming states for asymmetric swimmers—attractive, repulsive, and contracting-oscillatory, confirming that the expanding-oscillatory state reported in previous papers is not stable. The latter shows that there are rotative bound states in hydrodynamic scattering of the swimmers.

DOI: 10.1103/PhysRevE.85.061914 PACS number(s): 87.19.ru, 47.15.G−, 45.40.Ln

I. INTRODUCTION

Analysis of small-scale swimmers like biological microorganisms is an active research area in physics and nanotechnology [1]. The purpose of these researches is to construct microfluidic devices with ability of controlled swimming and delivery of nanometric cargos like drugs to inaccessible tissues of the human body [2]. Hydrodynamic interactions (HI) between these swimmers and other objects suspended in the ambient fluid play a key role in the dynamics of them and lead to interesting and complicated phenomena such as the synchronization [3], the hydrodynamic fluctuation [4], the active suspensions [5], and the attraction or alignment of microswimmers by rigid surfaces [6,7] and the attraction and repulsion of them to each other [8]. To understand these phenomena it is necessary to first understand how HI can affect the dynamics and kinematics of these swimmers known as *active swimmers*. There are a variety of examples for the active swimmers ranging from motile bacteria and cells [9] to recently developed magnetically actuated microrobots [10]. There are also passive particles in nature ranging from ordinary colloids to polymers [11].

Dynamics of the microswimmers is governed by low-Reynolds-number hydrodynamics in which the viscose forces dominate the inertia forces; therefore, the momentums are relaxed faster than any swimming period [12]. Swimming at low-Reynolds-numbers is subject to the *scallop theorem*, stating that a swimmer with one degree of freedom would not achieve a net translation in its swimming at viscose medium [13]. Purcell proposed a three-linked-sheet swimmer that could overcome the high viscose medium by *nonreciprocal* deformations [13]. Najafi and Golestanian proposed a simpler and more realizable model that consisted of three spheres linked by two arms [14]. The three-sphere swimmer propels itself by opening and closing of arms with a relative phase resulting in nonreciprocality of a period of the deformations. Despite simple shape, the three-sphere swimmer generates complicated flow field around itself, which is dominantly quadrupolar in the case of symmetric arms and dipolar in the case of asymmetric arms [8]. A three-sphere swimmer far from a rigid surface orients itself parallel to the surface [7]. Two three-sphere swimmers have complicated behavior in vicinity of each other [8]. The behavior of a double-swimmer system dramatically depends on the relative positions, orientations, and internal phases [8]. Two symmetric three-sphere swimmers moving in the same directions show four swimming states; attractive, repulsive, parallel, and oscillatory [8]. In scattering of three-sphere swimmers, the angle between their swimming directions will be preserved during the scattering process [15]. A point like sphere in vicinity of a three-sphere swimmer will trace closed loops [16].

Regarding the above-mentioned dynamical effects, in this paper, we investigate the HI between two three-sphere low-Reynolds-number swimmers by more detailed and precise calculations. The differential equations governing the dynamics of the incompressible creeping flow (low-Reynolds-number flow) are given by the Stokes equations as follows:

$$\begin{aligned} -\nabla p + \eta \nabla^2 \mathbf{u} &= \mathbf{0}, \\ \nabla \cdot \mathbf{u} &= \mathbf{0}, \end{aligned} \tag{1}$$

where η is the viscosity of the ambient fluid, $\mathbf{u}$ is the fluid flow field, and p is the pressure field. In this regime, the Reynolds number is low; i.e., $R = \rho L V/\eta \sim 0$, where ρ is the density of fluid, V is the velocity of swimmer, and L is the biggest dimension of the swimmer [12]. One of the fundamental solutions of Eq. (1) is flow due to a moving sphere, which can be represented as a point-force with strength $\mathbf{b}$ located at the center of sphere $\mathbf{x}_0$. The flow field around the point force can be represented by multiplication of a Green's function by the point force strength vector

$$u_i = \frac{1}{8\pi\eta} G_{ij}(\mathbf{x}, \mathbf{x}_0) b_j, \tag{2}$$

where $i, j = 1,2,3$ [12]. The Green's function can be calculated in several ways, one of which is represented in Ref. [12]. The Green's function is known as *Stokeslet* or *Oseen-Burger*

*farzin@znu.ac.ir

tensor, which is given as follows:

$$S_{ij} = \frac{\delta_{ij}}{r} + \frac{\hat{x}_i \hat{x}_j}{r^3},$$

where $r = |\hat{\mathbf{x}}|$, $\hat{\mathbf{x}} = \mathbf{x} - \mathbf{x}_0$, and $i, j = 1,2,3$ [17]. Note here that the *Faxen*'s relation implies the finite-size correction to the Green's function [12]. To calculate HI between the spheres suspended in a fluid, the *mobility* tensor is used whose elements are the Stoleslets. Applying the no-slip boundary conditions, implying that the fluid velocity is equal to the sphere velocity at the surface of sphere, to Eq. (2), the fluid velocity can be eliminated and replaced by the sphere velocity. Therefore, it is possible to expand the velocity of each sphere in terms of the hydrodynamic forces exerted on the other spheres [18],

$$\dot{\mathbf{x}}_i = \sum_{j=1}^{N} \mathbf{M}_{ij} \cdot \mathbf{f}_j, \tag{3}$$

where $i = 1,..,N$ and N is the number of spheres and $\mathbf{M}_{ij}$'s are the cross mobility tensors whose elements are the Stokeslets and $\mathbf{M}_{ii}$'s are the self-mobility tensors described by the Stokes friction coefficient $\mu = 1/6\pi\eta a$, where a is the radius of sphere. The linearity of these solutions arises from the linearity of the Stokes equations. In the following sections, we present details of the perturbation method as well as the numerical technique used in the calculations.

II. PERTURBATION METHOD

In this section, the standard perturbation method used to solve Eq. (3) written for two three-sphere low-Reynolds-number swimmers is described. We choose a three-dimensional frame of reference in which the fluid is stationary and swimmers are moving in the x-y plane. In this frame of reference, place of each sphere is specified by position vector $\mathbf{x}$ and orthogonal unit vectors $\mathbf{n}$ and $\mathbf{n}^{\perp}$ move with the swimmers. Body unit vectors are chosen such that $\mathbf{n}$ points to the swimming direction and $\mathbf{n}^{\perp}$ is perpendicular to it and points to the incremental direction of angle θ between swimming direction and positive x direction. In our notation, all of the quantities related to the second swimmer are indicated by a prime superscript.

Propulsion is due to opening and closing of arms. The front and back arms of the first swimmer are indicated by the following functions:

$$h(t) = L + u_1(t)$$
$$g(t) = L + u_2(t),$$

where L is equilibrium length of the arms and u_1 and u_2 are time-dependent functions indicating how arms oscillate. In fact, u's will determine the dynamics of swimmers. For a complete discussion on the u functions, see Ref. [19]. Among a wide variety of possible oscillatory functions, we choose the trigonometric functions to indicate arms oscillation as follows:

$$u_1(t) = \varepsilon_f \sin \omega t$$
$$u_2(t) = \varepsilon_b \sin(\omega t + \phi_0),$$

where ε_f and ε_b are oscillation amplitudes of the front and back arms, respectively, ω is the angular frequency of oscillation, and ϕ_0 is the relative phase of the front and back arms. Dynamics of the second swimmer is determined by u''s as follows:

$$u'_1(t) = \varepsilon'_f \sin(\omega t + \phi)$$
$$u'_2(t) = \varepsilon'_b \sin(\omega t + \phi_0 + \phi),$$

where, again, ε'_f and ε'_b are the oscillation amplitudes of the front and back arms, respectively, and ϕ is relative phase of two swimmers. Since the self-propelled particles are force-free and torque-free objects, we can apply the following constraints to the equations of motion:

$$\mathbf{f}_1 + \mathbf{f}_2 + \mathbf{f}_3 = \mathbf{0}$$
$$h\mathbf{n}^{\perp} \cdot \mathbf{f}_2 - g\mathbf{n}^{\perp} \cdot \mathbf{f}_3 = 0.$$

Force-free and torque-free conditions for the second swimmer are the same as the above equations but with primed quantities, so we do not repeat them for the sake of brevity. From Fig. 1, one can see that $\mathbf{x}_2 - \mathbf{x}_1 = h\mathbf{n}$ and $\mathbf{x}_1 - \mathbf{x}_3 = g\mathbf{n}$ hold. Using these expressions, $\mathbf{x}_2, \mathbf{x}_3, \mathbf{f}_1$, and $\mathbf{f}'_1$ can be eliminated in Eq. (3). Taking derivatives of the position vectors and keeping in mind that $\partial_t \mathbf{n} = \dot{\theta}\mathbf{n}^{\perp}$ and applying all constraints to Eq. (3), the following set of equations are obtained,

$$\begin{aligned}
\dot{\mathbf{x}}_1 + \dot{h}\mathbf{n} + h\dot{\theta}\mathbf{n}^{\perp} &= (\mathbf{M}_{22} - \mathbf{M}_{21}) \cdot \mathbf{f}_2 + (\mathbf{M}_{23} - \mathbf{M}_{21}) \cdot \mathbf{f}_3 + (\mathbf{M}_{22'} - \mathbf{M}_{21'}) \cdot \mathbf{f}'_2 + (\mathbf{M}_{23'} - \mathbf{M}_{21'}) \cdot \mathbf{f}'_3 \\
\dot{\mathbf{x}}_1 &= (\mathbf{M}_{12} - \mathbf{M}_{11}) \cdot \mathbf{f}_2 + (\mathbf{M}_{13} - \mathbf{M}_{11}) \cdot \mathbf{f}_3 + (\mathbf{M}_{12'} - \mathbf{M}_{11'}) \cdot \mathbf{f}'_2 + (\mathbf{M}_{13'} - \mathbf{M}_{11'}) \cdot \mathbf{f}'_3 \\
\dot{\mathbf{x}}_1 - \dot{g}\mathbf{n} - g\dot{\theta}\mathbf{n}^{\perp} &= (\mathbf{M}_{32} - \mathbf{M}_{31}) \cdot \mathbf{f}_2 + (\mathbf{M}_{33} - \mathbf{M}_{31}) \cdot \mathbf{f}_3 + (\mathbf{M}_{32'} - \mathbf{M}_{31'}) \cdot \mathbf{f}'_2 + (\mathbf{M}_{33'} - \mathbf{M}_{31'}) \cdot \mathbf{f}'_3.
\end{aligned} \tag{4}$$

Obtaining exact solutions of the above equations is a difficult task because the cross mobilities themselves contain the spheres' positions. However, we can use some approximation methods like the perturbation method to approach the exact solution. To solve these equations by the perturbation method, we need a perturbation parameter that should be small enough. If the swimmers are supposed to be far enough away from each other such that r is greater than the greatest dimension of the swimmer L, the choice of perturbation parameter as $\epsilon = L/r$ will be an appropriate one. Now, all of the quantities in the Eq. (4) should be expanded in terms of ϵ, e.g., $\mathbf{f} = \mathbf{f}^{(0)} + \epsilon\mathbf{f}^{(1)} + \epsilon^2\mathbf{f}^{(2)} + \cdots$ and so on. After multiplying all terms, each side of the equations is expanded as a power series in terms of ϵ. By equalizing the terms with the same power in ϵ and solving them, the velocities and forces are determined order-by-order. We note here that to solve the

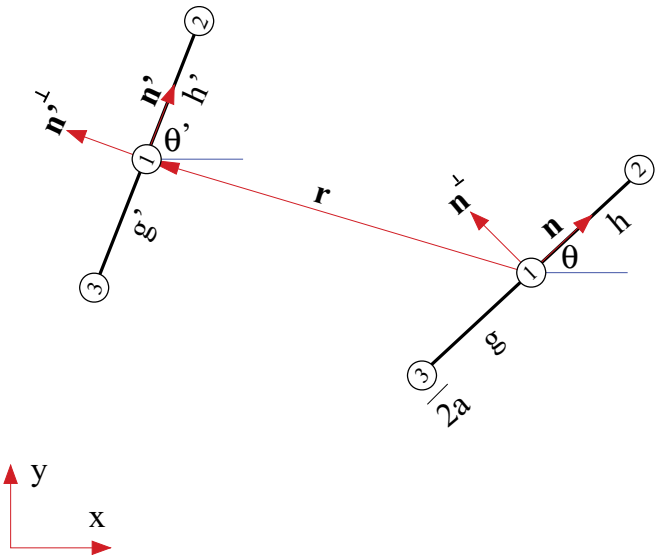

FIG. 1. (Color online) Schematic view of the three-sphere swimmers and parameters of the problem.

equations in each order of the perturbation, it is necessary to expand the denominators of the solutions in terms of small quantities a/L and u/L using the Taylor expansion, i.e., $(1+x)^n \sim 1+nx+n(n-1)x^2/2!+\cdots$. After expanding the denominators of the solutions, we obtain expressions in terms of multiplications of the u functions. Finally, the time-averaged solutions are calculated by integrating them over a complete period of deformations. Solutions of the perturbation method as well as the supporting numerical solutions are presented in Secs. IV, V, and VI. In the following section, we describe the details of numerical method used to solve Eq. (3) for three-sphere swimmers.

III. NUMERICAL METHOD

The second approximation method we use to solve the problem of HI between two swimmers is to solve Eq. (3) numerically. Note here that in the previous section only the equations of motion for the first swimmer are used in the perturbation method, while for the numerical calculation the equations of motion for all spheres are used. Discrete equations are obtained by writing Eq. (3) as follows:

$$\frac{\mathbf{x}_i(t+\Delta t)-\mathbf{x}_i(t)}{\Delta t}=\sum_{j=1}^{N}\mathbf{M}_{ij}(t)\cdot\mathbf{f}_j(t+\Delta t), \qquad (5)$$

where $i=1,N$. As it can be seen from Eq. (5), the position and forces are unknown at the same time. So bringing the forces to the left-hand side of Eq. (5) and all of known quantities to the right-hand side, we obtain a set of linear equations that can be written as

$$\mathbf{A}\cdot\mathbf{X}=\mathbf{B},$$

where the matrix $\mathbf{A}$ contains coefficients of unknown variables, the vector $\mathbf{X}$ contains unknown variables, and the vector $\mathbf{B}$ contains the known variables. For a free swimmer problem, a (7×7) and for a double swimmer problem, a (14×14) system of equations must be solved. Dimensionless quantities are set as $\tilde{x}=x/L$, $\tilde{t}=\omega t$, $\tilde{v}=v/L\omega$, and $\tilde{f}=f/L^2\omega\eta$. The time step is set to $\Delta\tilde{t}=10^{-4}$, which is optimized by an adapting step size method [20]. In our simulations we have set $\tilde{a}=0.1$, $\tilde{\varepsilon}=0.1$, and $\tilde{r}=100$. Note here that our calculations are in a noise-free regime. These conditions are satisfied for swimming in water at room temperature by setting $\omega\sim 1000Hz$ [21]. For implementing a fourth-order Runge-Kutta step, the set of equations should be solved four times in each time step [20]. In the following sections, perturbation results will be compared to numerical results for collinear swimmers. To this end, we run two computer programs; first we have calculated the forces and velocity of a free swimmer by solving a (7×7) set of equations and saved them for using in later calculations. Then, we have solved a (14×14) set of equations for the double-swimmer problem. Finally, the double-swimmer quantities are subtracted by the free-swimmer quantities. The resulting quantities are only due to the HI between two swimmers.

IV. HYDRODYNAMIC FORCES

The first quantities obtained from the perturbation method are the hydrodynamic forces exerted on each sphere. In the zeroth order, the time averaged self-propelling forces are given as

$$\begin{aligned}\mathbf{f}_1^{(0)}&=-\frac{5}{4}\pi\eta\frac{a^2}{L^2}\Phi_0\mathbf{n}\\ \mathbf{f}_2^{(0)}&=\frac{5}{8}\pi\eta\frac{a^2}{L^2}\Phi_0\mathbf{n}\\ \mathbf{f}_3^{(0)}&=\frac{5}{8}\pi\eta\frac{a^2}{L^2}\Phi_0\mathbf{n},\end{aligned} \qquad (6)$$

where $\Phi_0=\langle\dot{u}_1u_2-\dot{u}_2u_1\rangle=\varepsilon_b\varepsilon_f\omega\sin\phi_0$ is a function proportional to the area of configuration space from which the system is passed during a full period of deformations and $\langle\rangle$ indicates time average. As can be seen from Eq. (6) the middle sphere experiences a force opposite to the direction of swimming, which is a direct consequence of the force-free conditions. Numerical calculations show that $\tilde{f}_1=-4.3\times 10^{-4}$, while analytical results show that $\tilde{f}_1^{(0)}=-3.93\times 10^{-4}$. This difference is reasonable because the next term in the expansion of the zeroth order force would be a term like $C\pi\eta a^3\Phi_0/L^3$, with C a constant. Both the magnitude of this term and the difference between the analytical and numerical solutions are $O[10^{-5}]$. The first- and second-order corrections to the forces vanish; i.e., $\mathbf{f}_i^{(1)}=\mathbf{f}_i^{(2)}=0$. In the third order, the following terms survive from the time averaging process:

$$\begin{aligned}\mathbf{f}_1^{(3)}&=-\frac{3}{2}\pi\eta a^2L\Phi_1\left[\frac{\mathbf{D}\cdot\mathbf{n}}{r^3}\right]\mathbf{n}\\ \mathbf{f}_2^{(3)}&=\frac{3}{2}\pi\eta a^2L\Phi_2\left[\frac{\mathbf{D}\cdot\mathbf{n}}{r^3}\right]\mathbf{n}\\ \mathbf{f}_3^{(3)}&=-\frac{3}{2}\pi\eta a^2L\Phi_3\left[\frac{\mathbf{D}\cdot\mathbf{n}}{r^3}\right]\mathbf{n},\end{aligned} \qquad (7)$$

where we have

$$\begin{aligned}\Phi_1&=\langle(\dot{u}_1'+\dot{u}_2')(u_1-u_2)\rangle\\ \Phi_2&=\langle(\dot{u}_1'+\dot{u}_2')(2u_1+u_2)\rangle\\ \Phi_3&=\langle(\dot{u}_1'+\dot{u}_2')(u_1+2u_2)\rangle,\end{aligned}$$

by choosing the trigonometric functions for u's and time average, we have

$$\Phi_1 = \frac{\omega}{2}[(\varepsilon_b\varepsilon_b' - \varepsilon_f'\varepsilon_f)\sin\phi - (\varepsilon_b\varepsilon_f' + \varepsilon_f\varepsilon_b')\cos\phi]$$
$$\Phi_2 = \frac{\omega}{2}[(\varepsilon_b\varepsilon_f' - 2\varepsilon_b'\varepsilon_f)\cos\phi - (\varepsilon_b\varepsilon_b' + 2\varepsilon_f\varepsilon_f')\sin\phi]$$
$$\Phi_3 = \frac{\omega}{2}[(2\varepsilon_b\varepsilon_f' - \varepsilon_b'\varepsilon_f)\cos\phi - (2\varepsilon_b\varepsilon_b' + \varepsilon_f\varepsilon_f')\sin\phi].$$

Also, we have

$$\mathbf{D} = \Delta_1\mathbf{n} + 3(\hat{\mathbf{r}}\cdot\mathbf{n})\Delta_2\hat{\mathbf{r}} + 6\left[(\hat{\mathbf{r}}\cdot\mathbf{n}) - (\hat{\mathbf{r}}\cdot\mathbf{n}')(\mathbf{n}\cdot\mathbf{n}')\right]\hat{\mathbf{r}},$$

where $\Delta_1 = 1 - 3(\hat{\mathbf{r}}\cdot\mathbf{n}')^2$ and $\Delta_2 = 5(\hat{\mathbf{r}}\cdot\mathbf{n}')^2 - 3$, and so we have

$$\mathbf{D}\cdot\mathbf{n} = 1 - 3(\hat{\mathbf{r}}\cdot\mathbf{n})^2 - 3(\hat{\mathbf{r}}\cdot\mathbf{n}')^2 - 6(\mathbf{n}\cdot\mathbf{n}')(\hat{\mathbf{r}}\cdot\mathbf{n})(\hat{\mathbf{r}}\cdot\mathbf{n}') + 15(\hat{\mathbf{r}}\cdot\mathbf{n})^2(\hat{\mathbf{r}}\cdot\mathbf{n}')^2.$$

Clearly, one can see that the force-free conditions are not satisfied in Eq. (7). This effect arises because of presence of the second swimmer. The inner product $(\mathbf{D}\cdot\mathbf{n})$ has significance because it determines how force functions depend on the relative orientation of swimmers. It is clear that, in general, $(\mathbf{D}\cdot\mathbf{n}) > 0$. Absolutely, $(\mathbf{D}\cdot\mathbf{n})$ is invariant under the transformation $(\mathbf{n}\leftrightarrow\mathbf{n}')$. Furthermore, the third-order correction to the force arises from simultaneous swimming of two swimmers and are along the intrinsic swimming direction.

A typical comparison between the numerical and analytical results for third-order correction to the forces are shown in Fig. 2 in a situation that two symmetric swimmers approach together collinearly (the first swimmer moves to right and the second moves to left). In this graph, the hydrodynamic forces exerted on each sphere of the first swimmer are indicated in terms of the relative phase of swimmers. The numerical results are calculated using the procedure discussed in Sec. III and the analytical results are the third order forces, i.e., $\mathbf{f}_i^{(3)}$'s. Difference between the analytical and numerical results should be $\sim a^2\varepsilon^2(1+\cos\phi)/r^3$. This is the next term in the third-order perturbation expansion of forces. Choosing the parameters as $\tilde{r} = 100$ and $\phi = 0$, we will have the difference between two results up to $O[10^{-11}]$, so the difference which is seen in Fig. 2 is reasonable. Generally, Fig. 2 shows that the active HI between two collinear three-sphere swimmers are nonzero. In the case of distant swimmers, i.e., $\tilde{r} = 100$, the middle sphere experiences a force proportional to $\cos\phi$. This proportionality is predicted by Φ_1 function involved in $\mathbf{f}_1^{(3)}$. As swimmers getting closer, i.e., $\tilde{r} = 10$, the contribution of $\sin\phi$ will be getting more apparent. In the other words, in far distances the hydrodynamic force exerted on the middle sphere is invariant under the transformation $(\phi\leftrightarrow-\phi)$ but in near distances this invariance no longer holds. The side spheres experience the hydrodynamic forces as a linear combination of $\cos\phi$ and $\sin\phi$ such that the coefficient of sinusoidal function is greater than that of cosine function. Figure 2 indicates that in near distances the front sphere experiences a strong hydrodynamic force rather than the back sphere. This effect is more manifest in $(\phi < \pi)$.

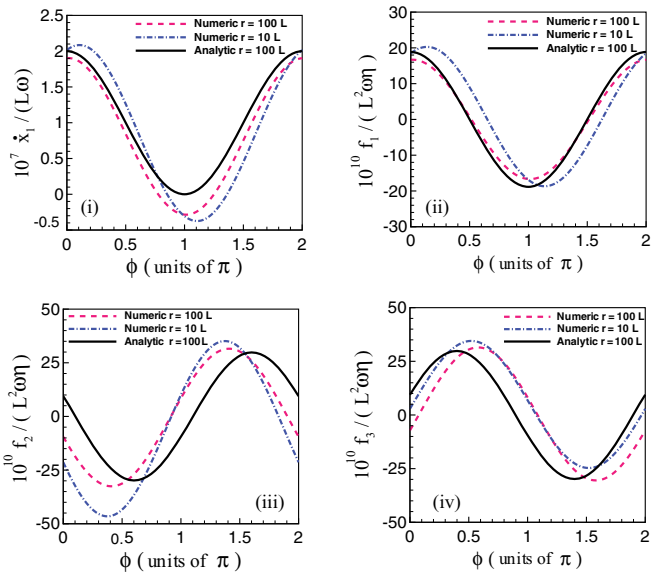

FIG. 2. (Color online) A comparison between the analytical and numerical results for the translational velocity and hydrodynamic forces. Two swimmers approach collinearly such that the first swimmer moves to the right and the second moves to the left. (i) The translational velocity of first swimmer in terms of relative phase of the swimmers; (ii), (iii), and (iv) are the hydrodynamic forces exerted on the first, second, and third spheres of the first swimmer, respectively. Black (solid) line: the third-order correction to the translational velocity and hydrodynamic forces at $\tilde{r} = 100$; red (dashed) line: the far field numerical results at $\tilde{r} = 100$; and blue (dash-dotted) line: the near field numerical results at $\tilde{r} = 10$.

In the fourth order, we find

$$\mathbf{f}_1^{(4)} = \frac{3}{2}\pi\eta a^2L^2\Phi_1\left[\frac{\mathbf{Q}\cdot\mathbf{n}^\perp}{r^4}\right]\mathbf{n}^\perp$$
$$\mathbf{f}_2^{(4)} = \frac{3}{2}\pi\eta a^2L^2\Phi_4\left[\frac{\mathbf{Q}\cdot\mathbf{n}^\perp}{r^4}\right]\mathbf{n}^\perp \qquad (8)$$
$$\mathbf{f}_3^{(4)} = -\frac{3}{2}\pi\eta a^2L^2\Phi_5\left[\frac{\mathbf{Q}\cdot\mathbf{n}^\perp}{r^4}\right]\mathbf{n}^\perp,$$

where we have

$$\Phi_4 = \langle(\dot{u}_1' + \dot{u}_2')(3u_1 + 4u_2)\rangle$$
$$\Phi_5 = \langle(\dot{u}_1' + \dot{u}_2')(4u_1 + 3u_2)\rangle,$$

and by choosing the trigonometric functions and time averaging over them, we arrive at the following expressions:

$$\Phi_4 = \frac{\omega}{2}[(4\varepsilon_b\varepsilon_f' - 3\varepsilon_b'\varepsilon_f)\cos\phi - (4\varepsilon_b\varepsilon_b' + 3\varepsilon_f\varepsilon_f')\sin\phi]$$
$$\Phi_5 = \frac{\omega}{2}[(3\varepsilon_b\varepsilon_f' - 4\varepsilon_b'\varepsilon_f)\cos\phi - (3\varepsilon_b\varepsilon_b' + 4\varepsilon_f\varepsilon_f')\sin\phi],$$

also we have

$$\mathbf{Q} = \{1 - 5(\hat{\mathbf{r}}\cdot\mathbf{n})^2 - 5(\hat{\mathbf{r}}\cdot\mathbf{n}')^2 + 2(\mathbf{n}\cdot\mathbf{n}')^2 - 20(\hat{\mathbf{r}}\cdot\mathbf{n})(\hat{\mathbf{r}}\cdot\mathbf{n}')(\mathbf{n}\cdot\mathbf{n}') + 35(\hat{\mathbf{r}}\cdot\mathbf{n})^2(\hat{\mathbf{r}}\cdot\mathbf{n}')^2\}\hat{\mathbf{r}}.$$

It is apparent that $\mathbf{Q}$ is always in the positive $\hat{\mathbf{r}}$ direction. One can see that $\mathbf{Q}$ is invariant under the transformation $(\mathbf{n}\leftrightarrow\mathbf{n}')$, so we can conclude that all vectors describing the simultaneous

swimming of the active swimmers are invariant under the replacement of swimmers.

V. TRANSLATIONAL VELOCITY

Using the forces obtained in the previous section, we calculate the translational velocity of the first swimmer. The zeroth order or self-propelling velocity is given as

$$\dot{\mathbf{x}}_1^{(0)} = \frac{7}{24}\frac{a}{L^2}\Phi_0\mathbf{n}. \tag{9}$$

The numerical result for the free swimmer by using the chosen parameters in Sec. III is $\tilde{\dot{x}}_1 = 3.18 \times 10^{-4}$ while $\tilde{\dot{x}}_1^{(0)} = 2.92 \times 10^{-4}$. The next term in the zeroth order perturbation is $\sim Ca^2\Phi_0/L^3$. The difference between the numerical and analytical results is $O[10^{-5}]$, which is to the order of the next term in expansion. Calculations show that the first-order velocity vanishes, i.e., $\dot{\mathbf{x}}_1^{(1)} = 0$. In the second order of perturbation, the leading order term reads as

$$\dot{\mathbf{x}}_1^{(2)} = \frac{27}{64}\frac{a}{L^2}\Phi_6\left[\frac{\Delta_1}{r^2}\hat{\mathbf{r}}\right], \tag{10}$$

where $\Phi_6 = \omega\varepsilon'_b\varepsilon'_f(\varepsilon'^2_b - \varepsilon'^2_f)$. This term vanishes when the second swimmer is symmetric, i.e., $\varepsilon'_b = \varepsilon'_f$, indicating that the asymmetric swimmers at far distances generate flow field dominantly similar to a point force dipole. The third-order velocity is given as

$$\dot{\mathbf{x}}_1^{(3)} = \frac{aL}{4}\Phi_1\left[\frac{\mathbf{D}\cdot\mathbf{n}}{r^3}\right]\mathbf{n} - \frac{aL}{2}\Phi'_0\left[\frac{\mathbf{T}}{r^3}\right], \tag{11}$$

where we have

$$\mathbf{T} = \tfrac{1}{2}\Delta_1\mathbf{n}' + 3(\hat{\mathbf{r}}\cdot\mathbf{n}')\Delta_2\hat{\mathbf{r}}.$$

The first term on the right-hand side of Eq. (11) corresponds to simultaneous swimming and the second term on the right-hand side corresponds only to the swimming of the second swimmer. Hence, we call the first term *active* and the second *passive*. However, a different result has been reported in Ref. [8] for the active term of the translational velocity. The essential difference is how the active term depends on the relative orientation of swimmers. Pooley and co-workers [8] report it as,

$$\dot{\mathbf{x}}_1^{(3)} \sim \left[\frac{\hat{\mathbf{r}} - (\hat{\mathbf{r}}\cdot\mathbf{n})\mathbf{n}}{r^3}\right] \times [(\hat{\mathbf{r}}\cdot\mathbf{n}) + 2(\mathbf{n}\cdot\mathbf{n}')(\hat{\mathbf{r}}\cdot\mathbf{n}') - 5(\hat{\mathbf{r}}\cdot\mathbf{n})(\hat{\mathbf{r}}\cdot\mathbf{n}')^2].$$

As it can be seen, this term has a component along $\mathbf{n}$ and one along $\hat{\mathbf{r}}$ while in Eq. (11) we have obtained only one component along $\mathbf{n}$. Also, the above expression does not satisfy the invariance under $(\mathbf{n} \leftrightarrow \mathbf{n}')$. The difference will be more apparent when two swimmers move collinearly in which $(\hat{\mathbf{r}}\cdot\mathbf{n}) = 1$ and $(\hat{\mathbf{r}}\cdot\mathbf{n}') = -1$. In this situation, the above expression vanishes while Eq. (11) does not. Also, in Fig. 2 numerical results confirm that the active interactions are nonzero when swimmers move collinearly. From Eq. (11) and the fact that $(\mathbf{D}\cdot\mathbf{n}) > 0$, it can be inferred that the active term of the translational velocity always pushes the swimmer in the intrinsic direction of swimming. Also, inspecting Eq. (11) for two in-phase collinear swimmers shows that two approaching swimmers attract each other and two swimmers going far away from each other repel each other. Therefore, this confirms that the three-sphere swimmer behaves like a pump or a jet.

Here, we are able to make a comparison between strength of each term of the translational velocity considering that the swimmers are similarly asymmetric, i.e., $(\varepsilon'_b = \varepsilon_b \neq \varepsilon_f = \varepsilon'_f)$. Comparing the dipolar and quadrupolar terms for a typical relative orientation of swimmers indicates that the active interactions between the asymmetric swimmers are dominant in the following distances:

$$r \leqslant \frac{32L^3}{27}\left|\frac{\cos\phi}{\varepsilon_b^2 - \varepsilon_f^2}\right|,$$

and the passive one in distances

$$r \leqslant \frac{32}{27}\frac{L^3}{|\varepsilon_b^2 - \varepsilon_f^2|}.$$

At distances greater than those mentioned above, the dipolar behavior dominates. So at distances in which the HI are important, there are the quadrupolar interactions playing the key role in the dynamics. This situation can be understood as quadrupolar screening of these swimmers that can be tuned by the relative phase of swimmers. This effect may be utilized to design and fabrication of the future man-made microswimmers.

VI. ANGULAR VELOCITY

The leading order term of the angular velocity of the first swimmer, i.e., $\dot{\boldsymbol{\theta}}$, survives from the fourth-order expansion and $\dot{\boldsymbol{\theta}}^{(0)}$, $\dot{\boldsymbol{\theta}}^{(1)}$, $\dot{\boldsymbol{\theta}}^{(2)}$, and $\dot{\boldsymbol{\theta}}^{(3)}$ vanish. The time-averaged angular velocity of first swimmer is given as

$$\dot{\boldsymbol{\theta}}^{(4)} = -\frac{21}{16}aL\Phi_1\left[\frac{\mathbf{Q}\cdot\mathbf{n}^{\perp}}{r^4}\right]\mathbf{n}^{\perp} - \frac{aL}{2}\Phi'_0\left[\frac{\mathbf{P}\cdot\mathbf{n}^{\perp}}{r^4}\right]\mathbf{n}^{\perp}, \tag{12}$$

where we have

$$\mathbf{P} = \left[\tfrac{1}{2}(\mathbf{n}\cdot\mathbf{n}')\Delta_3 + 3(\hat{\mathbf{r}}\cdot\mathbf{n}')(\hat{\mathbf{r}}\cdot\mathbf{n})\Delta_4\right]\hat{\mathbf{r}},$$

where $\Delta_3 = 39(\hat{\mathbf{r}}\cdot\mathbf{n}')^2 - 9$ and $\Delta_4 = 7 - 15(\hat{\mathbf{r}}\cdot\mathbf{n}')^2$. One can see that again there are active and passive terms on the right-hand side of Eq. (12). Apart from the numerical coefficient (21/16), the active term of the angular velocity in Eq. (12) confirms the result of Ref. [8]. From Eq. (12) and this fact that $\mathbf{Q}$ is always pointing to the positive $\hat{\mathbf{r}}$-direction, it can be shown that the active term of the angular velocity gives rise to rotation of the first swimmer in both clockwise and counter-clockwise directions. The former holds when the second swimmer is located over the first swimmer, i.e., $(\mathbf{Q}\cdot\mathbf{n}^{\perp}) > 0$, and the latter holds when the second swimmer is located under the first swimmer, i.e., $(\mathbf{Q}\cdot\mathbf{n}^{\perp}) < 0$. Thus, in general, the active term leads the swimmers to repel each other.

VII. SWIMMING IN THE SAME DIRECTIONS

In this section, we numerically investigate the long-time swimming paths of two swimmers when they are initially oriented in the same directions, i.e., $(\mathbf{n}\cdot\mathbf{n}') = 1$. For this end, the first swimmer is located in the origin of the reference

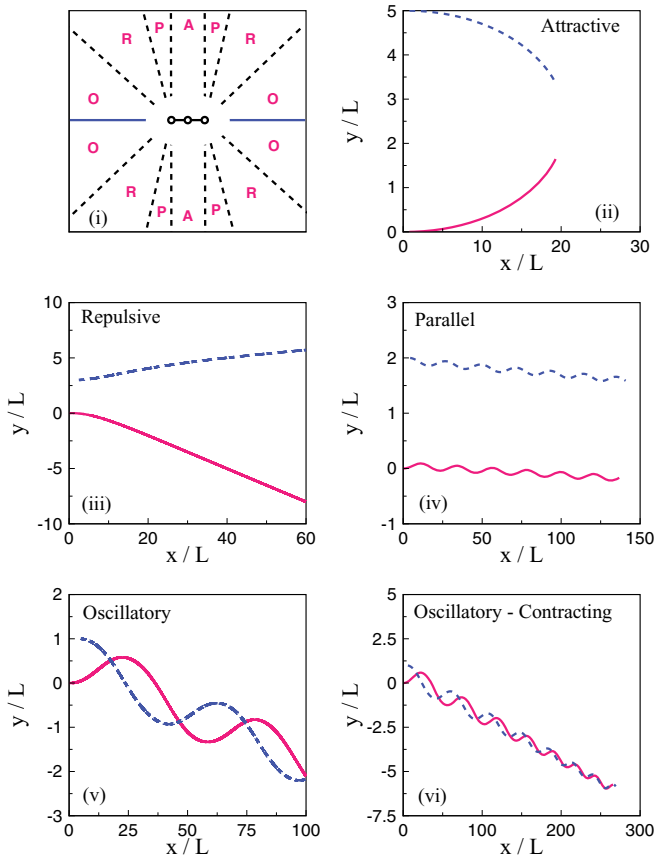

FIG. 3. (Color online) Long-time swimming states for two three-sphere swimmers moving in the same directions. (i) The area boundaries around the first swimmer each of which corresponding to different long-time swimming states; (ii) attractive, (iii) repulsive, (iv) parallel, (v) oscillatory, and (vi) oscillatory-contracting states. The red (solid) line is the trajectory of the first swimmer, and the blue (dashed) line is the trajectory of the second swimmer.

frame and the second one is located around it and then we let them swim for a long time. As discussed in Sec. III, for simulation of two swimmers it is necessary to solve a (14×14) set of equations. Here again the fourth-order Runge-Kutta method is utilized to make discrete equations and the time step is set to $(\Delta\tilde{t} = 10^{-4})$. Parameters of the problem are set such that the Oseen hydrodynamics is not violated, i.e., the spheres separation is $> \frac{3}{2}a$, hence for two symmetric swimmers we have set $\tilde{a} = 0.1$ and $\tilde{\varepsilon} = 0.1$. Simulations show that two symmetric swimmers have four different swimming states indicated in Fig. 3 as attractive, repulsive, parallel, and oscillatory states. The simulations also show that when the symmetry of swimmers is broken, the swimming states change as well. The changes occur such that the asymmetric swimmers will have only three swimming states; attractive, repulsive, and oscillatory-contracting states. In this situation, the parallel and oscillatory states are replaced by the oscillatory-contracting state. Also, it is observed that the asymmetric swimmers with $(\varepsilon_b < \varepsilon_f)$ and $(\varepsilon'_b > \varepsilon'_f)$ or $(\varepsilon_b > \varepsilon_f)$ and $(\varepsilon'_b < \varepsilon'_f)$ are contracted faster than the asymmetric swimmers with $(\varepsilon_b < \varepsilon_f)$ and $(\varepsilon'_b < \varepsilon'_f)$ or $(\varepsilon_b > \varepsilon_f)$ and $(\varepsilon'_b > \varepsilon'_f)$. In Ref. [8] it is mentioned that there is an oscillatory-expanding state for the asymmetric swimmers with $(\varepsilon'_b = \varepsilon_b > \varepsilon_f = \varepsilon'_f)$, in which the swimmers suddenly separate from each other after a few oscillatory motions. Our simulations show that this state is not stable. So, we can conclude that asymmetric low-Reynolds-number swimmers, e.g., *Escherichia coli* bacterium, hydrodynamically have a strong tendency for the cluster and chain formation observed in variety of motile cells aggregations [22–25].

VIII. SWIMMING IN THE OPPOSITE DIRECTIONS: HYDRODYNAMIC SCATTERING

In this section we numerically investigate the long-time behavior of two swimmers moving in opposite directions. The initial conditions are arranged such that the first swimmer is placed on the origin of the reference frame and the second one is placed in different positions on the vertical direction. The opposite swimming is made by setting $(\theta = 0)$ and $(\theta' = \pi)$. We let them swim for a long time and record their swimming paths. The outcome is very interesting because at near distances they rotate in the same directions over a circular path and then separate simultaneously [26]; see Fig. 4. Though the direction of swimming has been changed after separation, the angle between the swimming directions, i.e., $(\theta - \theta')$, is preserved. Also, simulations show that the smaller the collision parameter b, the bigger the scattering angles θ and θ'. The scattering gives rise to significant change of the swimming direction in some circumstances, for instance, Fig. 4(iv) shows the scattering with $(\theta > \pi/2)$ for the collision parameter $(\tilde{b} = 0.67)$. Therefore, the hydrodynamic scattering of two active low-Reynolds-number swimmers can lead to form unidirectional rotative bound states arising from strong hydrodynamic coupling of swimmers at near distances.

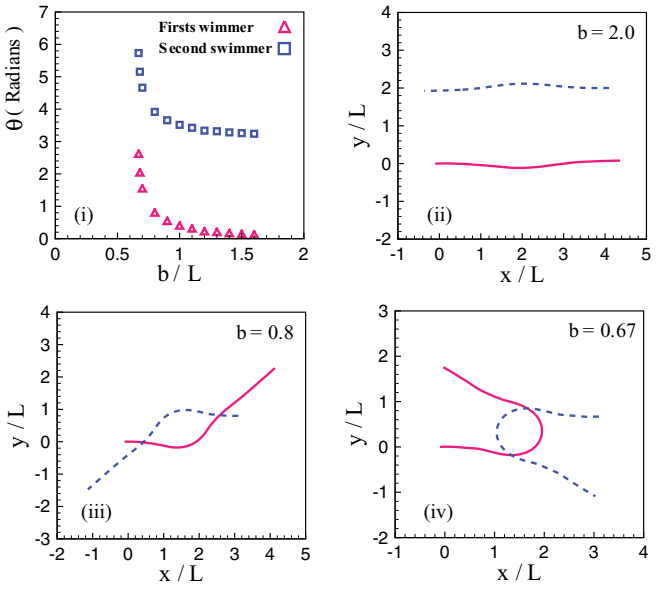

FIG. 4. (Color online) Long-time swimming behavior of two three-sphere swimmers moving in the opposite directions. (i) Collision parameter b in terms of the scattering angle θ. (ii) A glancing collision without any significant change in the swimming directions. (iii) A hard collision with $\theta < \pi/2$. (iv) A hard collision with $\theta > \pi/2$. The red (solid) line is the trajectory of the first swimmer and the blue (dashed) line is the trajectory of the second swimmer.

IX. CONCLUDING REMARKS

In this paper we study the HI between the three-sphere swimmers at low-Reynolds-numbers by using the analytical calculations and numerical simulations. In Sec. IV the hydrodynamic forces exerted on a free-swimmer were calculated and it was shown that a free swimmer experiences the hydrodynamic forces along its intrinsic swimming direction. A symmetric swimmer forms a point-force quadrupole, which at far distances generates a flow field proportional to r^{-3}, while an asymmetric swimmer forms a point force dipole with a flow field proportional to r^{-2}. Both the hydrodynamic forces and translational velocity of a free swimmer are proportional to Φ_0, i.e., the area enclosed in the configuration space, which in turn depends on the oscillation amplitudes ε_b and ε_f and the relative phase of arms. In the double-swimmer problem, the forces have two components parallel and perpendicular to swimmers, but the parallel forces $\sim r^{-3}$ are stronger than the perpendicular one $\sim r^{-4}$. Nevertheless, the weak perpendicular forces cause significant dynamical effects on the swimmers. The translational and angular velocities in the double-swimmer problem are calculated in the next step, indicating that these quantities consist of a passive and an active term. The passive terms are only due to swimming of the second swimmer, while the active terms are originated from simultaneous swimming of both swimmers. The active terms are invariant under the transformation ($\mathbf{n} \leftrightarrow \mathbf{n}'$), but the passive terms are not. Analytical calculations demonstrate that the active term of the translational velocity is along the intrinsic direction of swimming and does not vanish when two swimmers move collinearly, and these results are supported by numerical calculations. The significance of this result is that there are many circumstances in nature that biological microorganisms move collinearly, for example, in blood vessels and other thin channel-shaped tissues of the body. Hence, it is important to know whether they sense the active HI, or in other words, the relative phase of swimming. Also, to construct the future artificial swimmers with the ability of controlled swimming, it should be noted that the active interactions play a more significant role rather than the passive one; thus, many of phenomena like cluster and chain formation in the bacterial suspensions are due to active nature of mutual interactions.

Also, we investigated the long-time swimming paths of two swimmers in two general initial conditions—swimming in the same and opposite directions. In the former situation, two symmetric swimmers show four different swimming states—attractive, repulsive, parallel, and oscillatory—while two asymmetric swimmers show only three swimming states—attractive, repulsive, and contracting-oscillatory. The contracting-oscillatory state demonstrates that the asymmetric microswimmers are drastically forced to form clusters and chains, a phenomenon that has been frequently observed in nature [22,23]. In the latter situation, two swimmers are entered to a hydrodynamic scattering in which they rotate in the same directions and then separate. During the occurrence of this effect, the angle between the swimming directions is preserved for the symmetric swimmers.

[1] H. Bruss, *Theoretical Microfluidics* (Oxford University Press, Oxford, 2008).

[2] S. H. Kim, J. H. Jeong, S. H. Lee, S. W. Kim, and T. G. Park, J. Controlled Release **129**, 107 (2008).

[3] A. Najafi and R. Golestanian, Europhys. Lett. **90**, 68003 (2010).

[4] R. A. Simha and S. Ramaswamy, Phys. Rev. Lett. **89**, 058101 (2002).

[5] C. Hohenegger and M. J. Shelley, Phys. Rev. E **81**, 046311 (2010).

[6] A. P. Berke, L. Turner, H. C. Berg, and E. Lauga, Phys. Rev. Lett. **101**, 038102 (2008).

[7] R. Zargar, A. Najafi, and M. F. Miri, Phys. Rev. E **80**, 026308 (2009).

[8] C. M. Pooley, G. P. Alexander, and J. M. Yeomans, Phys. Rev. Lett. **99**, 228103 (2007).

[9] P. Nelson, *Biological Physics* (W. H. Freeman and Company, New York, 2004).

[10] R. Dreyfus, J. Baudry, M. L. Roper, M. Fermigier, H. A. Stone, and J. Bibette, Nature (London) **862**, 437 (2005).

[11] M. Doi and S. F. Edwards, *The Theory of Polymer Dynamics* (Oxford University Press, Oxford, 1986).

[12] C. Pozrikidis, *Introduction to Theoretical and Computational Fluid Dynamics* (Cambridge University Press, Cambridge, 1992).

[13] E. M. Purcell, Am. J. Phys. **45**, 3 (1977).

[14] A. Najafi and R. Golestanian, Phys. Rev. E **69**, 062901 (2004).

[15] G. P. Alexander, C. M. Pooley, and J. M. Yeomans, Phys. Rev. E **78**, 045302 (2008).

[16] J. Dunkel, V. B. Putz, I. M. Ziad, and J. M. Yeomans, Soft Matter **6**, 4268 (2010).

[17] C. W. Oseen, *Neuere Methoden und Ergebniss in der Hydrodynamik* (Akademishe Verlagsgesellschaft, Leipzig, 1927).

[18] S. H. Rad and A. Najafi, Phys. Rev. E **82**, 036305 (2010).

[19] R. Golestanian and A. Ajdari, Phys. Rev. E **77**, 036308 (2008).

[20] W. H. Press, S. A. Teukolsky, W. T. Vetterling, and B. P. Flannery, *Numerical Recipes in Fortran 77* (Cambridge University Press, Cambridge, 1992).

[21] A. Najafi, Phys. Rev. E **83**, 060902 (2011).

[22] E. Ben-Jacob, I. Cohen, and H. Levine, Adv. Phys. **49**, 395 (2000).

[23] I. H. Riedel, K. Kruse, and J. Howard, Science **309**, 300 (2005).

[24] X. Chen, X. Dong, A. Beer, H. L. Swinney, and H. P. Zhang, Phys. Rev. Lett. **108**, 148101 (2012).

[25] F. Peruani, J. Starruss, V. Jakovljevic, L. Sogaard-Andersen, A. Deutsch, and M. Bar, Phys. Rev. Lett. **108**, 098102 (2012).

[26] See Supplemental Material at http://link.aps.org/supplemental/10.1103/PhysRevE.85.061914 for an animating movie showing a typical hydrodynamic scattering between two three-sphere swimmers at low-Reynolds-numbers.